Int J Mech Mater Des (2014) 10:379–394
DOI 10.1007/s10999-014-9253-2

Adjoint design sensitivity analysis of molecular dynamics in parallel computing environment

Hong-Lae Jang · Jae-Hyun Kim · Youmie Park · Seonho Cho

Received: 1 November 2013 / Accepted: 26 April 2014 / Published online: 14 May 2014

Abstract An adjoint design sensitivity analysis method is developed for molecular dynamics using a parallel computing scheme of spatial decomposition in both response and design sensitivity analyses to enhance the computational efficiency. Molecular dynamics is a path-dependent transient dynamic problem with many design variables of high nonlinearity. Adjoint variable method is not appropriate for path-dependent problems but employed in this paper since the path is readily available from response analysis. The required adjoint system is derived as a terminal value problem. To compute the interaction forces between atoms in different spatial boxes, only atomic positions in the neighboring boxes are required to minimize the amount of data communications. Through some numerical examples, the high nonlinearity of the selected design variables is discussed. Also, the accuracy of the derived adjoint design sensitivity is verified by comparing with finite difference sensitivity and the efficiency of parallel adjoint variable method is demonstrated.

Keywords Adjoint design sensitivity analysis · Molecular dynamics · Parallel computation · Path-dependent problem · Terminal value problem · Lennard–Jones potential

H.-L. Jang · J.-H. Kim · Y. Park · S. Cho (✉)
Department of Naval Architecture and Ocean Engineering, National Creative Research Initiatives (NCRI) Center for Isogeometric Optimal Design, Seoul National University, 1 Gwanak-ro, Gwanak-gu, Seoul 151-744, Korea
e-mail: secho@snu.ac.kr

H.-L. Jang
e-mail: perr83@snu.ac.kr

J.-H. Kim
e-mail: priuss1@snu.ac.kr

Y. Park
e-mail: youmiep@inje.ac.kr

Y. Park
College of Pharmacy, Inje University, Gimhae, Gyeongnam 621-749, Korea

1 Introduction

Recently, nanotechnology is one of the emerging research fields to describe the modern engineering problems such as nanoscale sensors, ultra-strength materials, drug delivery design, and so on. Therefore, interest in considering the design in a microscopic level is naturally increasing. The molecular dynamics (MD) simulation that predicts the microscopic behaviors of materials is a promising tool that is able to describe complex physical phenomena. However, a vast amount of computation is required for the transient dynamic analysis in atomic based simulations. The MD simulations are computationally large in both spatial and temporal domains. The length scale for atomic coordinates is angstroms and many thousands or millions of atoms must be simulated in

three dimensions to obtain the desired complex macroscopic phenomena. Also, the time step size is constrained by the periodicity of atomic vibration. This limits the unit of time steps to the femtosecond scale and therefore tens or hundreds of thousands of time steps are necessary to be evaluated for the real time simulation. For computational efficiency, the MD simulation is used only in the localized region of interest whereas the continuum analysis is carried out in the remaining region. Thus, using the MD simulation and the continuum analysis, many researchers have solved the problems of dislocation (Tadmor et al. 1996), crack propagation (Park et al. 2005; Farrell et al. 2007), and strain localization (Kadowaki and Liu 2004). When it comes to the field of design optimization, finite difference sensitivity for the transient dynamics is computationally costly but too inaccurate to be used in the design optimization. Many researchers developed the algorithms of MD simulation in parallel computing environment. Plimpton (Plimpton 1995) presented the parallel algorithms for short-range interaction molecular dynamics. The parallel algorithms for MD simulation are limited in the interaction force ranges. Solids and liquids are often modeled by using this short-range force only due to electronic screening effects or to avoid the computational cost of including long-range forces for simplicity.

The purpose of design sensitivity analysis (DSA) in MD simulations is three folds; (1) Instead of using the expensive first-principle quantum-mechanical (QM) method, the sensitivities of atomic mass m and L–J parameter ϵ, σ can be utilized to develop an empirical interatomic potential. Related studies are found in Mendelev et al. (2003). The design sensitivities of MD simulation can be utilized for the validation of force field parameters for the prediction of desired nanoscale phenomena compared with experimental data. (2) It can be utilized in the uncertainty quantification of MD systems. Instead of the popular Monte Carlo simulation that is a sampling-based approach for the sensitivity, the accurate and efficient adjoint sensitivity can be employed. (3) Due to the huge costs for the analysis of MD systems, the gradient-based approach and parallel computation indispensable for the design optimization of nanoscale materials, which are so far not developed yet but essential for the future direction of design optimization. In this paper, the parallel DSA of MD system is studied as a pioneering research, which can be later used to determine the optimal morphology of molecular structures such as nanoparticles for drug delivery, carbon nanotubes for material design, and so on. Also, the design sensitivities of MD simulation can be utilized for the validation of force field parameters for the prediction of desired nanoscale phenomena compared with experimental data.

Even though the MD is performed in parallel computing environment, there still remain some problems for the design sensitivity analysis (DSA) of MD simulations. From the computational point of view, the approximated DSA methods such as finite difference method are impractical for the efficiency and accuracy of design sensitivity since the MD simulation usually includes many highly nonlinear design parameters. Thus, very efficient analytical DSA methods are indispensable for the design optimization of MD systems using the MD simulations. The adjoint variable method (AVM) for the transient dynamics is well established and the corresponding adjoint system turned out to be a terminal value problem (Choi and Kim 2005). To recover the initial conditions correctly, the invertibility of the MD problem is required to solve the terminal value problem. Different from the notion of reversibility, the meaning of invertibility is that the evolution operator of dynamics has an inverse operator. Since the velocity Verlet algorithm is one of the Verlet version integrators and is employed in this research, the invertibility of the problem is guaranteed during the time evolution of the MD system (Strogatz 1994; Tuckerman et al. 1992).

Dynamic problems require the time integration of partial differential equations to compute dynamics responses. For the DSA of dynamic problems, the time-history of design sensitivity of state variables is required to calculate the sensitivity at a given time t. For such path dependent problems, the history of design sensitivity over loading paths is needed up to the load level at which the sensitivity is desired. The response sensitivity at a given time and position depends on both response and response sensitivities of all the previous time steps and locations of the structure. In other words, the exact paths of response and its sensitivity are needed. Thus, the AVM is not appropriate for path-dependent problems because each adjoint solution yields the sensitivity of only one performance measure, rather than the sensitivities of the full response fields (Cho and Choi 2000a). For transient dynamic problems with large deformation elastic-plastic materials, an analytical DSA method

(Cho and Choi 2000b) is developed in the updated Lagrangian formulation using the direct differentiation method (DDM). Hsieh and Arora (1984) developed DSA methods for the dynamic problems of point-wise constraints; the DDM and the AVM were used in their research. Tortorelli et al. (1989) derived the design sensitivity for nonlinear transient thermal systems, based on the adjoint approach using the Lagrange multiplier method and the convolution theory. Tsay and Arora (1990) derived nonlinear DSA for path-dependent problems in the frame of total Lagrangian formulation considering both geometrical and material nonlinearities. Gao et al. (2008) performed shape optimization for time-dependent Navier–Stokes flows. They used the Piola transformation to bypass the divergence-free condition for the shape DSA. In the MD system in this paper, we kept only the time history of kinematics for all the atoms since the tangent stiffness can be easily recovered directly from the original responses.

Extension of DSA methods to the atomic level transient dynamics was never attempted due to the limitation of computational resources and lack of efficient DSA method even though the MD simulations were already established. When the performance measure is only dependent on the terminal time state and the internal force term is linear with respect to the displacement due to the harmonic approximation of the inter-atomic potential, the adjoint equation of motion can be independently solved from the original system. In that case, there is an advantage of saving the computational storage to keep the original response history (Kim et al. 2013a, b) . In the case of non-linear internal forces, however, the adjoint equations depend on the path of original responses and thus the tangent stiffness in the adjoint systems changes with each time. In this case, the adjoint problem is time history dependent, which means that we must follow all the history of response analysis for solving that problem.

The remainder of this paper is organized as follows, in Sect. 2, we review the MD theory, which includes the discussion of equations of motion together with an inter-atomic potential. In Sect. 3, we discuss the DSA of MD, where both the DDM and the AVM are considered. The AVM is effective especially for the path-independent problems of many design variables but the MD in this research is a path-dependent problem. Thus a special treatment is required to apply the AVM to the MD problems. Also, a parallel computing scheme is introduced since a massive computation is generally required in the MD simulations. For computational efficiency, the parallel computing based on the spatial decomposition method is performed in both response analysis and the DSA. In Sect. 4, we present demonstrative numerical examples, where the accuracy and efficiency of the derived adjoint design sensitivity are discussed by comparing them with the finite difference method (FDM), which presents the importance of DSA in the MD simulations.

2 Review of molecular dynamics

2.1 Equations of motion

From the difference of kinetic energy and potential energy, a Lagrangian is defined, in Cartesian coordinates, as

$$L = \frac{1}{2}\sum_{i=1}^{N_a} m_i \dot{\mathbf{r}}_i \cdot \dot{\mathbf{r}}_i - U(\mathbf{r}_1, \mathbf{r}_2, \ldots, \mathbf{r}_{N_a}), \tag{1}$$

where $\mathbf{r}_i = (x_i, y_i, z_i)$ is the position vector of atom i in 3-dimensional space; the dot denotes time derivatives; m_i is the mass of atom i; U is an inter-atomic potential; and N_a is the total number of atoms. The following Euler–Lagrange equations,

$$\frac{d}{dt}\frac{\partial L}{\partial \dot{\mathbf{r}}_i} - \frac{\partial L}{\partial \mathbf{r}_i} = 0,\ i = 1, 2, \ldots, N_a, \tag{2}$$

lead to the equations of motion as

$$m_i \ddot{\mathbf{r}}_i = -\frac{\partial U(\mathbf{r}_1, \mathbf{r}_2, \ldots, \mathbf{r}_{N_a})}{\partial \mathbf{r}_i} \equiv \mathbf{f}_i,\ i = 1, 2, \ldots, N_a, \tag{3}$$

where $\mathbf{f}_i$ is the internal force exerted on atom i.

2.2 Inter-atomic potential

To describe accurate atomic interactions within the simulated system, we consider the subatomic nature of complicated quantum effects that are responsible for the bonding and breaking of atoms and the spatial arrangement of atomic valence. For the reliable results from MD simulations, the classical inter-atomic potential should include these quantum mechanical processes. A general structure of potential energy can be expressed as

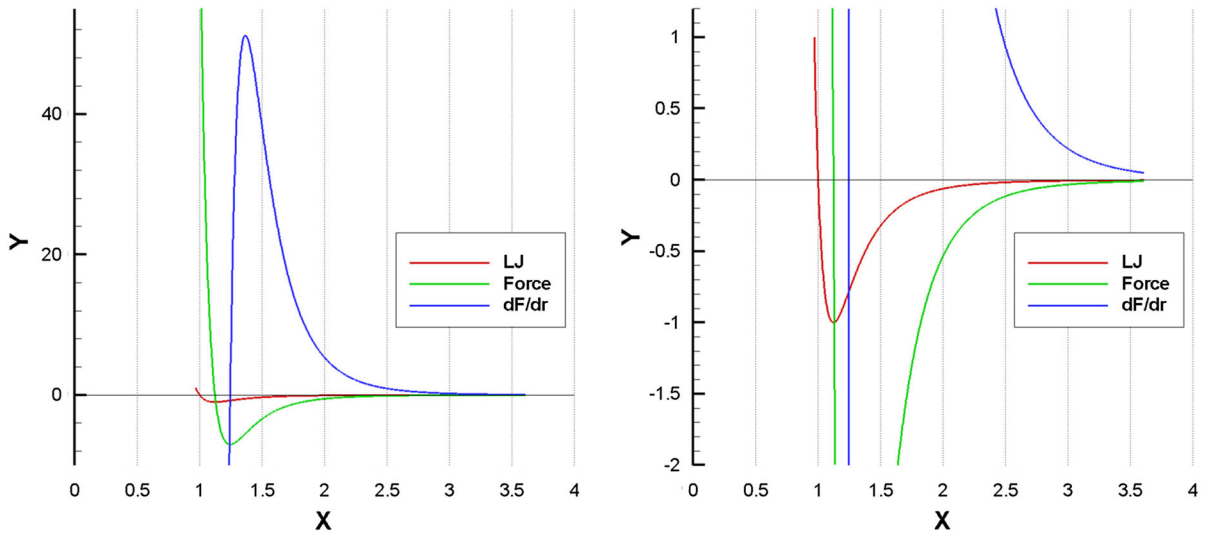

Fig. 1 L–J potential (*red*), L–J force (*green*), and the derivative of force (*blue*). (Color figure online)

$$U(\mathbf{r}_1,\mathbf{r}_2,\ldots\mathbf{r}_N) = \sum_i \Phi^1(\mathbf{r}_i) + \sum_{i,j>i} \Phi^2(\mathbf{r}_i,\mathbf{r}_j) + \sum_{i,j>i,k>j} \Phi^3(\mathbf{r}_i,\mathbf{r}_j,\mathbf{r}_k) + \cdots \tag{4}$$

where Φ^m is the m-body potential (Liu et al. 2006); the first term is the potential energy due to the gravity and the electrostatic force; the second term is due to the pair-wise interactions of particles; and the third is due to the three-body inter-atomic potential energy. Generally, the pair-wise interaction is employed, truncating the sum of Eq. (4) after the second term. Figure 1 shows the behavior of potential, its force, and the derivative of force for a general Lenard–Jones (LJ) potential. The potential is instead designed to include the multi-body effects in the pair-wise potential Φ^2.

In the crystalline solid structures, there is no bonding between atoms and the motion of atoms occurs near equilibrium position almost always. Thus, we can use the harmonically approximated expression of potential energy, by truncating the higher order terms and using the Taylor expansion of potential energy at equilibrium distance $r = r_0$, as

$$\Phi(r) \cong \Phi^h(r) = \frac{1}{2}k(r-r_0)^2 + \Phi(r_0), \tag{5}$$

where k is the stiffness between the atoms. Black and Bopp simulated the face centered cubic (FCC) metals for obtaining surface mode frequencies (Black and Bopp 1984). In their simulation, for the interactions between metal molecules, a harmonically approximated potential is used only on the nearest neighbors. Spohr and Heinzinger also used the harmonically approximated potential for the metal-metal interactions in their water/metal interaction simulation (Spohr and Heinzinger 1986).

3 DSA of molecular dynamics

3.1 Time-reversal symmetry in dynamics systems

In the dynamic problems, an adjoint equation is usually given as a terminal value problem and the initial conditions can be recovered according to the time reversibility of the system. A reversible system (or time reversal symmetry) is defined as any second-order system that is invariant under the reversed time and velocity ($t \to -t$ and $v \to -v$). Only the initial conditions, not the equations, can differ in the *"reversed flow"* of the reversible system (Strogatz 1994; Lamb and Roberts 1998). To investigate the characteristics of adjoint system in dynamics problems, consider a simple one-dimensional dynamic system with initial conditions,

$$\ddot{u}(t) + au(t) = 0,\ u(0) = u_0,\ \dot{u}(0) = v_0,\ 0 \le t \le t_T, \tag{6}$$

and a design sensitivity system with initial conditions,

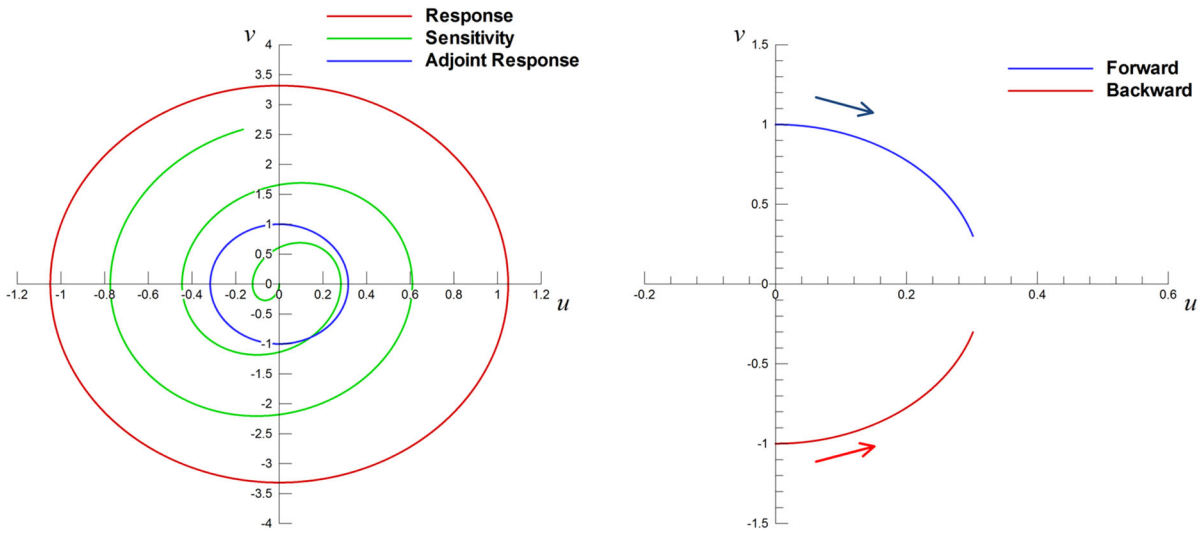

Fig. 2 Phase trajectories of original response, adjoint response, and sensitivity. (Color figure online)

$$\ddot{u}'(t) + au'(t) = -a'u(t),$$
$$u'(0) = 0,\ \dot{u}'(0) = 0,\ 0 \le t \le t_T. \tag{7}$$

The system governed by Eq. (6) is conservative and reversible. The design variable is a and the performance measure is the displacement $u(t_T)$ at terminal time. Figure 2(L) shows the phase trajectories of original response, adjoint response, and the sensitivity of the reversible system. In this case, $u_0 = 1.0$, $v_0 = 1.0$, $t_T = 50,000\Delta t$, and $\Delta t = 10^{-4}$. Since both original and adjoint systems possess the time-reversal symmetry, the trajectories of systems are symmetric about u-axis. However, the sensitivity trajectory is not symmetric due to the history-dependent force in the sensitivity equation. Figure 2(R) shows the procedure of solving the adjoint terminal value problem of the reversible system, where the trajectory of adjoint response is shown until the terminal time step of 4,000.

The red curve represents the actual trajectory of adjoint response by solving the terminal value problem with $\lambda(t_T) = 0.0,\ \dot{\lambda}(t_T) = -1.0$. The blue curve shows the trajectory of the adjoint response by solving the initial value problem with $\lambda(0) = 0.0,\ \dot{\lambda}(0) = 1.0$. In the trajectories of blue and red curves, since the adjoint system is reversible, the histories of displacement are identical but those of velocity are identical in magnitude but different in sign. With the reversed sign of adjoint velocity in the blue curve, the adjoint system is regarded as an initial value problem. Figure 3 shows the time histories of original and adjoint responses in forward direction. The adjoint system is identical to the original system except the initial conditions and thus has the same frequencies.

3.2 Adjoint variable method

From Eq. (3) for MD systems, the equations of motion can be written, in a matrix-vector form, as

$$\mathbf{M}_A(\mathbf{b})\ddot{\mathbf{u}} = \mathbf{f}(\mathbf{b}, \mathbf{u}), \tag{8}$$

where $\mathbf{M}_A$, $\mathbf{u}$, and $\mathbf{b}$ are the atomic mass matrix, displacement vector, and design variable vector, respectively. The term $\mathbf{f}(\mathbf{b}, \mathbf{u}) = -\partial U(\mathbf{b}, \mathbf{u})/\partial \mathbf{u}$ is the interaction force calculated from the potential energy $U(\mathbf{b}, \mathbf{u})$. Taking the first order variation of Eq. (8) with respect to the design $\mathbf{b}$ leads to the following design sensitivity equation

$$\mathbf{M}_A(\mathbf{b})\ddot{\mathbf{u}}' - \frac{\partial \mathbf{f}(\mathbf{b}, \mathbf{u})}{\partial \mathbf{u}}\mathbf{u}' = -\frac{\partial \mathbf{M}_A(\mathbf{b})}{\partial \mathbf{b}}\delta\mathbf{b}\ddot{\mathbf{u}} + \frac{\partial \mathbf{f}(\mathbf{b}, \mathbf{u})}{\partial \mathbf{b}}\delta\mathbf{b} \tag{9}$$

Since the initial conditions are independent of design, the corresponding initial conditions for the design sensitivity are selected as

$$\mathbf{u}'(0) = \dot{\mathbf{u}}'(0) = \mathbf{0} \tag{10}$$

For a general performance measure ψ that could include both terminal value and time history quantity for the MD system,

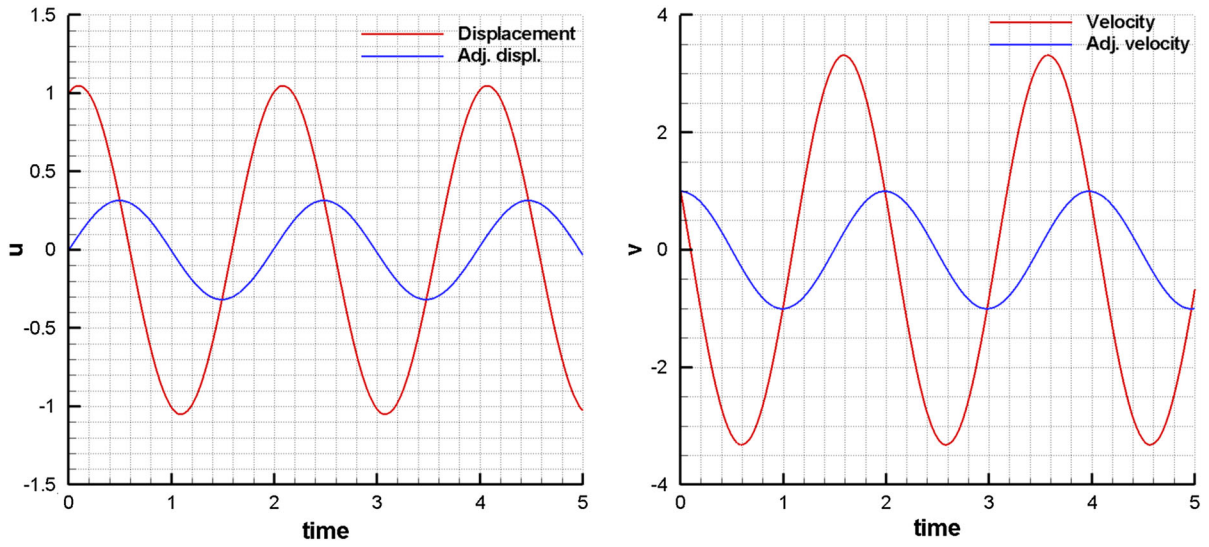

Fig. 3 Original and adjoint responses: (L) displacement, (R) velocity. (Color figure online)

$$\psi = g(\mathbf{b}, \mathbf{u}, \dot{\mathbf{u}})|_{t=t_T} + \int_0^{t_T} h(\mathbf{b}, \mathbf{u}, \dot{\mathbf{u}}) dt \tag{11}$$

taking the first order variation of Equation (11) with respect to the design $\mathbf{b}$ and integrating the last term in the integrand by parts lead to

$$\begin{aligned} \psi' &= \left(\frac{\partial g}{\partial \mathbf{b}} \delta \mathbf{b} + \frac{\partial g}{\partial \mathbf{u}} \mathbf{u}' + \frac{\partial g}{\partial \dot{\mathbf{u}}} \dot{\mathbf{u}}' \right) \Big|_{t=t_T} \\ &\quad + \int_0^{t_T} \left(\frac{\partial h}{\partial \mathbf{b}} \delta \mathbf{b} + \frac{\partial h}{\partial \mathbf{u}} \mathbf{u}' + \frac{\partial h}{\partial \dot{\mathbf{u}} \dot{\mathbf{u}}'} \right) dt \\ &= \left\{ \frac{\partial g}{\partial \mathbf{b}} \delta \mathbf{b} + \left(\frac{\partial g}{\partial \mathbf{u}} + \frac{\partial h}{\partial \dot{\mathbf{u}}} \right) \mathbf{u}' + \frac{\partial g}{\partial \dot{\mathbf{u}}} \dot{\mathbf{u}}' \right\} \Big|_{t=t_T} \\ &\quad + \int_0^{t_T} \left\{ \frac{\partial h}{\partial \mathbf{b}} \delta \mathbf{b} + \left(\frac{\partial h}{\partial \mathbf{u}} - \frac{d}{dt} \frac{\partial h}{\partial \dot{\mathbf{u}}} \right) \mathbf{u}' \right\} dt \end{aligned} \tag{12}$$

For the Lagrange multiplier function λ, the equation of motion should hold for all time spans.

$$\int_0^{t_T} \lambda^T (\mathbf{M}_A(\mathbf{b}) \ddot{\mathbf{u}} - \mathbf{f}(\mathbf{b}, \mathbf{u})) dt = 0 \tag{13}$$

Assuming that the Lagrange multiplier function or adjoint response λ is independent of design $\mathbf{b}$, the first order variation of Eq. (13) is obtained as

$$\begin{aligned} &\int_0^{t_T} \lambda^T \left(\frac{\partial \mathbf{M}_A(\mathbf{b})}{\partial \mathbf{b}} \delta \mathbf{b} \ddot{\mathbf{u}} + \mathbf{M}_A(\mathbf{b}) \ddot{\mathbf{u}}' - \frac{\partial \mathbf{f}(\mathbf{b}, \mathbf{u})}{\partial \mathbf{b}} \delta \mathbf{b} \right. \\ &\left. - \frac{\partial \mathbf{f}(\mathbf{b}, \mathbf{u})}{\partial \mathbf{u}} \mathbf{u}' \right) dt = 0 \end{aligned} \tag{14}$$

Integration by parts and using the initial conditions $\mathbf{u}'(0) = \dot{\mathbf{u}}'(0) = 0$, we obtain the following.

$$\begin{aligned} &\left(\lambda^T \mathbf{M}_A \dot{\mathbf{u}}' - \dot{\lambda}^T \mathbf{M}_A \mathbf{u}' \right) \Big|_{t=t_T} \\ &\quad + \int_0^{t_T} \left(\ddot{\lambda}^T \mathbf{M}_A - \lambda^T \frac{\partial \mathbf{f}(\mathbf{b}, \mathbf{u})}{\partial \mathbf{u}} \right) \mathbf{u}' dt \\ &\quad = - \int_0^{t_T} \lambda^T \left(\frac{\partial \mathbf{M}_A}{\partial \mathbf{b}} \ddot{\mathbf{u}} - \frac{\partial \mathbf{f}(\mathbf{b}, \mathbf{u})}{\partial \mathbf{b}} \right) \delta \mathbf{b} dt \end{aligned} \tag{15}$$

Comparing Eq. (15) with (12), an adjoint system is defined as

$$\mathbf{M}_A(\mathbf{b}) \ddot{\lambda} - \frac{\partial \mathbf{f}(\mathbf{b}, \mathbf{u})}{\partial \mathbf{u}} \lambda = \left(\frac{\partial h}{\partial \mathbf{u}} - \frac{d}{dt} \frac{\partial h}{\partial \dot{\mathbf{u}}} \right)^T \tag{16}$$

where the corresponding terminal conditions are given as

$$\lambda(t_T) = \mathbf{M}_A^{-1}(\mathbf{b}) \frac{\partial g^T}{\partial \dot{\mathbf{u}}} \text{ and } \dot{\lambda}(t_T) = -\mathbf{M}_A^{-1}(\mathbf{b}) \left(\frac{\partial g}{\partial \mathbf{u}} + \frac{\partial h}{\partial \dot{\mathbf{u}}} \right)^T \tag{17}$$

Thus, the adjoint design sensitivity can be obtained by using the analysis and adjoint responses,

$$\psi' = \frac{\partial g}{\partial \mathbf{b}} \delta \mathbf{b} \Big|_{t=t_T} + \int_0^{t_T} \left\{ \frac{\partial h}{\partial \mathbf{b}} - \lambda^T \left(\frac{\partial \mathbf{M}_A}{\partial \mathbf{b}} \ddot{\mathbf{u}} - \frac{\partial \mathbf{f}(\mathbf{b}, \mathbf{u})}{\partial \mathbf{b}} \right) \right\} \delta \mathbf{b} dt \tag{18}$$

Thus, the design sensitivity of general performance measure can be obtained using the original response in Equation (8) and the adjoint response in Eq. (16) with the terminal conditions of Eq. (17). In the MD system in this paper, we kept only the time history of kinematics for all the atoms since the tangent stiffness can be easily recovered directly from the original responses. For the time integration of adjoint system in Eq. (16), we kept only the displacement $\mathbf{u}(t)$ and velocity $\dot{\mathbf{u}}(t)$ histories of response. So that the tangent $\partial \mathbf{f}(\mathbf{b}, \mathbf{u})/\partial \mathbf{u}$ and adjoint load $(\partial h/\partial \mathbf{u} - (d/dt)(\partial h/\partial \dot{\mathbf{u}}))^T$ in Eq. (16) are successfully recovered using the saved displacement and velocity at every time step in backward direction. Note that if the adjoint system is reversible, we can obtain the adjoint response by time integrating the adjoint system in forward direction by changing the sign of the terminal velocity. Even if the original MD system has time reversal symmetry, the time reversibility of adjoint system is not related to the reversibility of the original one but to the type of performance measure.

3.3 Parallel computation

For short-range molecular dynamics, three parallel algorithms are presented by Plimpton (1995). To each processor, *the atomic decomposition method* assigns a fixed subset of atoms; *the force decomposition method* does a fixed subset of inter-atomic forces; and *the spatial decomposition method* does a fixed spatial region. The arithmetic and communication costs of each method are listed in Table 1, where N and p denote the numbers of atoms and processors, respectively.

3.3.1 The spatial decomposition method

For the parallel processing of MD simulations with short-range interactions, we generally employ the spatial decomposition method such that a processor has the position information of atoms in each spatial box to evaluate the kinematics of atoms. Thus, the interaction forces in each spatial box are easily obtained from the position of internal atoms. Also, to compute the interaction forces between atoms in different spatial boxes, we need the position information of atoms in nearby boxes which is readily available.

Table 1 Comparison of parallel computation costs

Decomposition method	Arithmetic cost	Communication cost
Atomic	$O(N/p)$	$O(N)$
Force	$O(N/p)$	$O(N/\sqrt{p})$
Spatial	$O(N/p)$	$O(N/p)$

In the MD simulations using the spatial decomposition method, it is impossible to balance the number of atoms and the computation loads in each processor since some of the atoms could leave or enter the processor. However, the spatial decomposition method has advantage of reducing the communication costs; it requires data communications with at most 26 neighboring processors in three-dimensional simulation if the length of spatial box in each processor is larger than the cut-off radius. For a single time step, the algorithm is shown in Fig. 4. Step (1) sends the kinematics and other identifying information for the atoms leaving the box. Steps (1) (2) are processed at the initial time-step but need not be done at each time-step. Step (3) separately computes the forces at each node, which do not require the communication of force data and thus reduce the communication costs. However, duplicated force computations could occur at the atoms on the boundary of subdomain. Step (4) updates the position information of atoms using the obtained forces. Step (5) requires six communications to obtain the position information of atoms in the neighboring processors.

The communication scheme we use to acquire the positions of neighboring atoms is illustrated in Fig. 5. The data communication occurs in the horizontal direction. If the length of box (L) is longer than the cut-off radius (r_c) for short range interactions, the processor communicates with only one adjacent processor. However, if L is smaller than r_c, each processor exchanges data with more than one adjacent processor. Next, data exchanges in the vertical

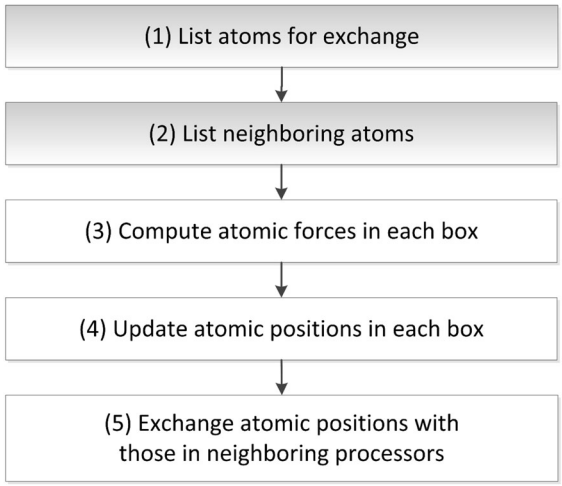

Fig. 4 Computing steps for a single time-step in spatial decomposition

direction occur in a similar way. Thus, for 3-dimensional problems, we can complete all data exchanges within just 6 data exchanges. More detailed algorithm for the data exchanges can be referred in the reference (Plimpton 1995). In this simulation, L is determined to be larger than r_c, $r_c < L$. There are three advantages to this scheme; *first*, when $r_c < L$, the necessary positions of atoms from all 26 surrounding boxes are efficiently obtained in just 6 data exchanges; *second*, when $r_c > L$, more distant boxes are necessary for the position information of atoms but only a few extra data exchanges are required; *third*, the amount of data communicated is minimized as shown in Table 1.

For the design sensitivity analysis, the spatial decomposition method is applicable and requires the position and its sensitivity information from the neighboring processors. Also, the same spatial decomposition method as used in the MD simulation is applicable for the MD simulation of adjoint system by substituting the forces with the adjoint loads.

4 Numerical examples

The aim of this chapter is to verify the accuracy and efficiency of the proposed adjoint DSA method. The L–J 6–12 potential is employed for the interactions between atoms as

$$U(r) = 4\varepsilon\left\{\left(\frac{\sigma}{r}\right)^{12} - \left(\frac{\sigma}{r}\right)^{6}\right\}, \tag{19}$$

where $r = \left|\mathbf{r}_i - \mathbf{r}_j\right|$ and ε is the energy depth which shows the bonding/dislocation of particles; the work required to be done in order to remove one of two coupled atoms from its equilibrium position. This means that the value of ε is the minimum value of Eq. (19). σ is the collision diameter; the distance at which $U(r) = 0$ and related with the equilibrium bond length. The equilibrium length is found such that the following inter-atomic force is equal to zero. The velocity Verlet algorithm is employed for the temporal integration scheme since it can provide displacement and velocity information at the same time.

Even though the atomic level simulation parameters like atomic mass are not physically controllable, we selected the parameters like atomic mass, energy depth, and collision diameter as the design variables for the purpose of what-if study. From the viewpoint of convergence and efficiency in MD simulations, it is very important to determine the appropriate size of time steps, which is dependent upon the highest vibration period of molecules or the material property. To ensure the stability of numerical scheme, the size of time steps is usually taken as 1 fs ($\Delta t = 10^{-3}\,(ps) = 1(fs)$) together with some safety factors, which is explained in detail in the reference (Leach 2001) For the parallel version of MD simulation and DSA, the massage passing interface (MPI) library is used. A cluster including 8 processors of Intel Xeon 3.0 GHZ and 4 GB memory in each node is used.

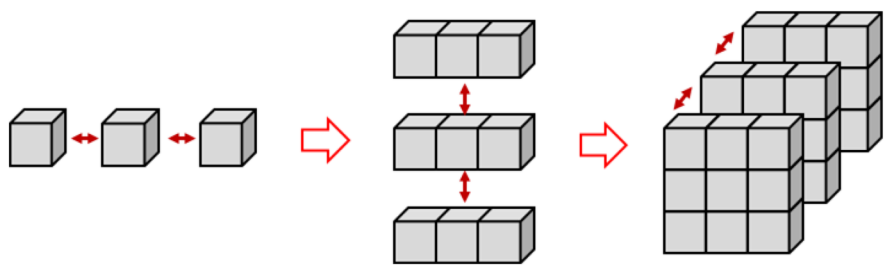

Fig. 5 Data exchange of all atom positions in adjacent boxes

4.1 Efficient and accurate computation of sensitivity

For the DSA of MD simulations, one of the big issues is the efficiency of sensitivity computation. To investigate the relevant factors, consider an argon gas model, whose simulation parameters are listed in Table 2. The specification of computing hardware includes 64bit Intel® Quadcore™(8 thread) i7 CPU 3.20 GHz with 24 GB memory. The MPICH is employed as a parallel tool.

4.1.1 Cut-off radius for efficiency

We consider a simple model of relatively small size to verify the derived adjoint sensitivity expression in Eqs. (16)–(18) and to check if the communication between nodes is working properly in parallel computing. To make the problem as simple as possible, we consider a simple cubic model of 512 argon atoms in Fig. 6., with all the mathematical idealizations such as periodic boundary condition and cut-off radius eliminated. The reference step size for this MD simulation is $\Delta t = 10^{-3}\,(ps) = 1(fs)$ (Leach 2001). However, the step size is multiplied by a safety factor of $1/10$ to ensure the numerical stability of design sensitivity equation and the parallel computing algorithm. The total number of time steps is determined as 10,000. The atomic mass (m), energy depth (ε), and collision diameter (σ) are selected as the design variables ($\mathbf{b}$). The amount of design perturbation for the FDM is $\delta\mathbf{b} = 10^{-4}\cdot\mathbf{b}$. In Table 3, the analytical sensitivities by the DDM and AVM are compared with the FDM at the time step of 10,000. The lower and upper rows in each design variable correspond to the results with and without considering the cut-off radius (2.5σ), respectively. Although the cut-off radius is introduced, it turns out that the sensitivity agreements are still very good. The computation of inter-atomic forces from the L–J potential is the most time-consuming process. If the number of atoms is equal to N and the cut-off radius is not considered, $N(N-1)/2$ computations are required. Using the L–J potential in Eq. (19), the inter-atomic force for *i-th* atom is computed as

$$\mathbf{f}_i^{Analysis} = \frac{\partial U(r)}{\partial r_i} = \sum_{j\neq i} \frac{24\varepsilon}{\sigma^2}\left\{2\left(\frac{\sigma}{r_{ij}}\right)^{14} - \left(\frac{\sigma}{r_{ij}}\right)^{8}\right\}\cdot\mathbf{r}_{ij}. \tag{20}$$

For the DDM, the right-hand side of the sensitivity equation in Eq. (9) is computed as

$$\begin{aligned}\mathbf{f}_i^{DDM} &= \frac{\partial\mathbf{f}(\mathbf{b},\mathbf{u})}{\partial\mathbf{u}_i}\mathbf{u}'_i - \frac{\partial\mathbf{M}_A(\mathbf{b})}{\partial\mathbf{b}}\delta\mathbf{b}\ddot{\mathbf{u}}_i + \frac{\partial\mathbf{f}(\mathbf{b},\mathbf{u})}{\partial\mathbf{b}}\delta\mathbf{b}\\ &= \sum_{j\neq i}\frac{24\varepsilon}{\sigma^2}\left[\left\{2\left(\frac{\sigma}{r}\right)^{14} - \left(\frac{\sigma}{r}\right)^{8}\right\} - \frac{8}{\sigma^2}\left\{\frac{7}{2}\left(\frac{\sigma}{r}\right)^{16} - \left(\frac{\sigma}{r}\right)^{10}\right\}\begin{pmatrix} r_x{}^2 & r_xr_y & r_xr_z\\ r_xr_y & r_y{}^2 & r_yr_z\\ r_xr_z & r_yr_z & r_z{}^2\end{pmatrix}\right]\cdot\left(\mathbf{u}'_i - \mathbf{u}'_j\right)\\ &\quad - \frac{\partial m}{\partial\mathbf{b}}\delta\mathbf{b}\ddot{\mathbf{u}}_i + \sum_{j\neq i}\frac{\partial\left[\frac{24\varepsilon}{\sigma^2}\left\{2\left(\frac{\sigma}{r}\right)^{14} - \left(\frac{\sigma}{r}\right)^{8}\right\}\right]}{\partial\mathbf{b}}\delta\mathbf{b}\cdot\mathbf{r}_{ij}\end{aligned} \tag{21}$$

For the AVM, the adjoint load in Eq. (16) is computed as

$$\begin{aligned}\mathbf{f}_i^{AVM} &= \frac{\partial\mathbf{f}(\mathbf{b},\mathbf{u})}{\partial\mathbf{u}}\lambda + \left(\frac{\partial h}{\partial\mathbf{u}} - \frac{d}{dt}\frac{\partial h}{\partial\dot{\mathbf{u}}}\right)^T\\ &= \sum_{j\neq i}\frac{24\varepsilon}{\sigma^2}\left[\left\{2\left(\frac{\sigma}{r}\right)^{14} - \left(\frac{\sigma}{r}\right)^{8}\right\} - \frac{8}{\sigma^2}\left\{\frac{7}{2}\left(\frac{\sigma}{r}\right)^{16} - \left(\frac{\sigma}{r}\right)^{10}\right\}\begin{pmatrix} r_x{}^2 & r_xr_y & r_xr_z\\ r_xr_y & r_y{}^2 & r_yr_z\\ r_xr_z & r_yr_z & r_z{}^2\end{pmatrix}\right]\cdot\left(\lambda_i - \lambda_j\right)\end{aligned} \tag{22}$$

Table 2 Simulation parameters

Density	ρ	1.428 (g/cm^2)
Initial temperature	T_0	180 (K)
Energy depth	ε	1.656×10^{-3} (aJ)
Collision diameter	σ	0.3405 (nm)
Atomic mass	m	66.34×10^{-3}(ykg)
Cut-off radius	r_c	$2.5\,\sigma$

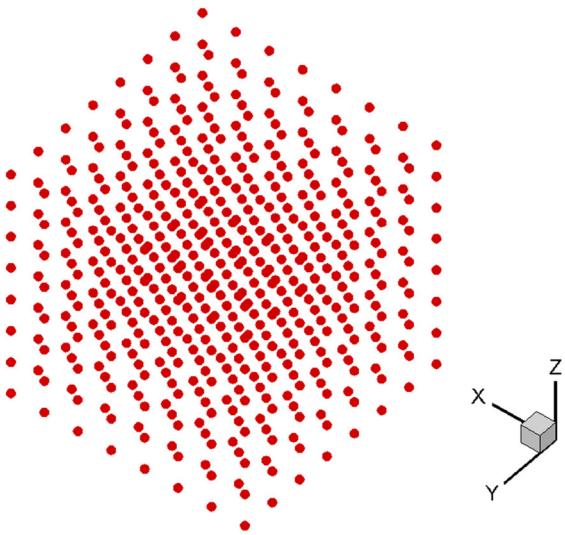

Fig. 6 Initial position of argon atoms

Therefore, if the cut-off radius is not used, the DDM requires significant computing costs. When the cut-off radius is not considered, the analytical sensitivities show excellent agreements but require more computation time than the finite difference sensitivity as shown in Table 4. In the problem of small design variables (3 in this example), the FDM turns out to be more efficient. When the cut-off radius ($r_c = 2.5\sigma$) is considered, however, the time for analysis (Analysis, FDM) is significantly reduced by 60 % of the original analysis time. The time for analytical sensitivities (DDM, AVM) is much more reduced by 85 %.

4.1.2 *High nonlinearity of design variables*

The argon gas model in Fig. 7 is initially a simple cubic structure consisting of 10,648 atoms with 31,944 DOFs. Using the step size of time $\Delta t = 10^{-3}$ (ps), the dynamic system is integrated during 10,000 time steps and the diffusion phenomenon due to the initial room temperature is successfully simulated as shown in Fig. 7.

The computational costs for MD simulation, DDM, and AVM are compared according to the number of processors in parallel computing environment as shown in Fig. 8. All the costs are normalized by the MD simulation time with a single processor (182 minutes). When eight processors are used for the MD simulation and the DSA, the computational costs are reduced to 1/4 of the cost when using a single processor. Consider the diffusivity as a performance measure at terminal time.

$$\psi = D(\mathbf{u}, \dot{\mathbf{u}}) = \frac{1}{6N_A}\frac{d}{dt}\left(\mathbf{u}^T\mathbf{u}\right)\Big|_{t=t_T} = \frac{1}{3N_A}\mathbf{u}^T\dot{\mathbf{u}}\big|_{t=t_T}. \tag{23}$$

The mass of all atoms m, energy depth ε, and collision diameter σ are selected as the design variables. The amount of design perturbation for the FDM is $\delta\mathbf{b} = 10^{-9} \cdot \mathbf{b}$. To demonstrate the accuracy of analytical DSA method, we compared the sensitivities obtained from FDM (a), DDM (b), and AVM (c) as shown in Table 5. The upper, middle, and lower rows in each design variable correspond to the results at the time steps of 100, 1,000, and 10,000, respectively. Compared with the FDM, the analytical DSA methods yield very accurate results. Even though the perturbation amount is 10^{-7} % of initial design, the agreement

Table 3 Comparison of various sensitivity results

DV	(a) FDM	(b) DDM	(c) AVM	$(b)/(a) \times 100\,\%$	$(c)/(a) \times 100\,\%$	$(c)/(b) \times 100\%$
m	1.137764E − 01	1.137834E − 01	1.137834E − 01	100.006	100.006	100.000
	1.042371E − 01	1.046488E − 01	1.046488E − 01	100.395	100.395	100.000
ε	−4.563737E + 00	−4.563915E + 00	−4.563915E + 00	100.004	100.004	100.000
	−4.160074E + 00	−4.197521E + 00	−4.197521E + 00	100.900	100.900	100.000
σ	3.813301E − 01	3.805748E − 01	3.805748E − 01	99.802	99.802	100.000
	4.319947E − 01	4.226014E − 01	4.226014E − 01	97.826	97.826	100.000

Table 4 Comparison of computation time ($t_T = 10,000\Delta t$)

Method	No cut-off radius		Cut-off radius		
	Time	Normalized	Time	Normalized	Reduction (%)
Analysis	259.217	1.00	104.0215	1.00	59.87
DDM	3790.659	14.62	555.7848	5.34	85.34
AVM	1351.722	5.21	206.7793	1.99	84.70
FDM	763.077	2.94	309.9272	2.98	59.38

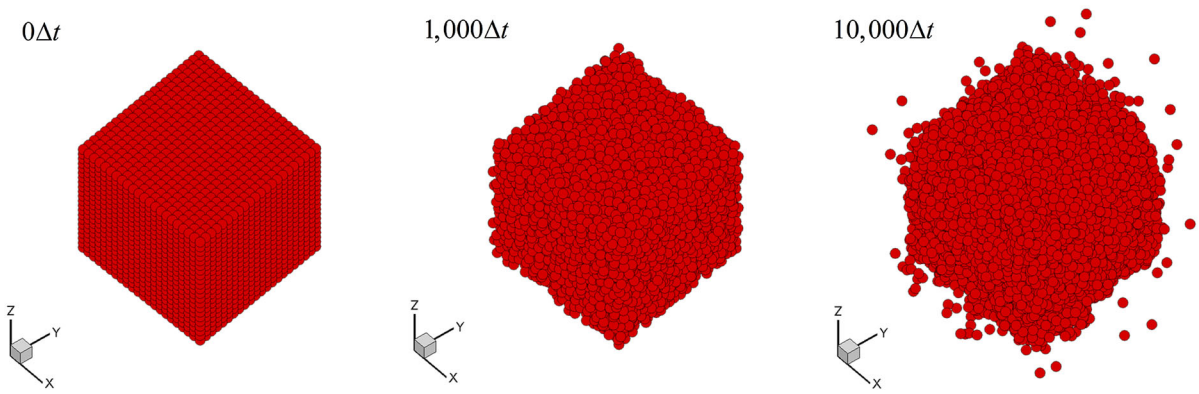

Fig. 7 Simulation of argon gas diffusion

between the analytical and the numerical sensitivities of collision diameter σ gets slightly worse as the terminal time increases. This is due to the high nonlinearity of L-J parameter σ in Eq. (16) with respect to the response as well as the design. To investigate the nonlinearity of the design variables, consider the performance measure of time-averaged temperature which is given as

$$\psi = \frac{1}{t_T}\int_0^{t_T}\left(\frac{m\dot{\mathbf{u}}(t)^T\dot{\mathbf{u}}(t)}{N_{dof}\cdot N_a\cdot k_B}\right)dt, \tag{24}$$

where N_{dof}, N_a, and k_B are the number of DOFs per atom, the number of atoms, and Bolzman constant, respectively. The following L–J potential and harmonic potential are used.

$$U_{LJ}(r) = 4\varepsilon\left(\left(\frac{\sigma}{r}\right)^{12} - \left(\frac{\sigma}{r}\right)^{6}\right),$$
$$U_h = U_{LJ}(r_0) + \frac{18\sqrt[3]{4}\varepsilon}{\sigma^2}(r - r_0)^2. \tag{25}$$

In this numerical test, we concentrate only on the accuracy of analytical sensitivity for highly nonlinear

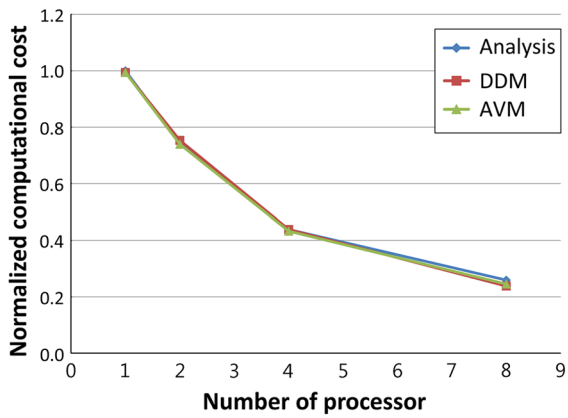

Fig. 8 Reduction of computational costs. (Color figure online)

design variables. The step size of time is sufficiently reduced to $\Delta t = 10^{-5}$ to prevent possible numerical instability. The dynamic system is integrated for 200 time steps. The collision diameter σ is selected as a design variable. Figure 9 shows the percentage difference between the FDM and DDM results according to the variation of perturbation amount in FDM. The harmonic potential is less dependent on the

Table 5 Comparison of sensitivities at time steps of $t_T = 100\Delta t,\ 1000\Delta t,\ 10000\Delta t$

DV	(a) FDM	(b) DDM	(c) AVM	$(c)/(a) \times 100\%$
m	1.423496E−02	1.423599E−02	1.423599E−02	100.007
	3.942760E−02	3.944201E−02	3.944201E−02	100.037
	−1.484524E+03	−1.476054E+03	−1.476054E+03	99.429
ε	−5.709744E−01	−5.709737E−01	−5.709737E−01	100.000
	−1.581463E+00	−1.581463E+00	−1.581463E+00	100.000
	5.888401E+04	5.921489E+04	5.921489E+04	100.562
σ	−4.038140E−02	−4.038140E−02	−4.038140E−02	100.000
	2.451670E−01	2.451669E−01	2.451669E−01	100.000
	6.511735E+03	7.235908E+03	7.235908E+03	111.121

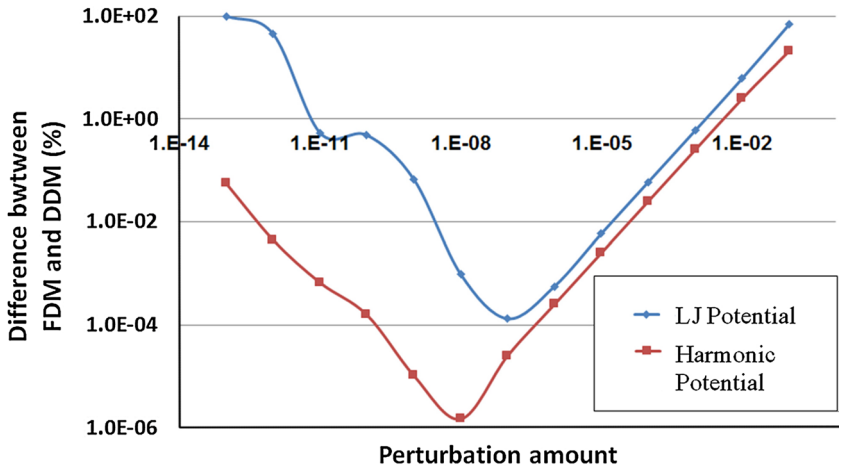

Fig. 9 Linearity test for FDM using various potentials. (Color figure online)

Table 6 Linearity test for FDM with respect to perturbation amount

$\delta\sigma/\sigma$	(a)FDM	(b)DDM	(c)AVM	$(b)/(a) \times 100\,\%$	$(c)/(a) \times 100\,\%$
1.00E−02	2.146732E+03			83.629	83.632
1.00E−04	1.860049E+03			96.519	96.522
1.00E−06	1.859400E+03			96.553	96.555
1.00E−08	1.883083E+03	1.795298E+03	1.795351E+03	95.338	95.341
1.00E−10	1.795296E+03			100.000	100.003
1.00E−12	1.794449E+03			100.047	100.050
1.00E−14	1.702798E+03			105.432	105.435

perturbation amount than the L–J potential. The finite difference sensitivity changes significantly depending on the design perturbation amount as shown in Table 6 when the system is integrated up to 1,000 time steps. Since the potential we employ is highly nonlinear with respect to the collision diameter in the Eq. (25), perturbation that is either too big or too small could cause inaccurate sensitivity for the FDM. These results show that the analytical DSA methods are indispensable in MD simulations.

4.2 Nano film subjected to impulsive displacement

Consider a thin film consisting of *NDV* layers, which is subjected to an impulse of $v_0 = 10\ (nm/ps)$ as

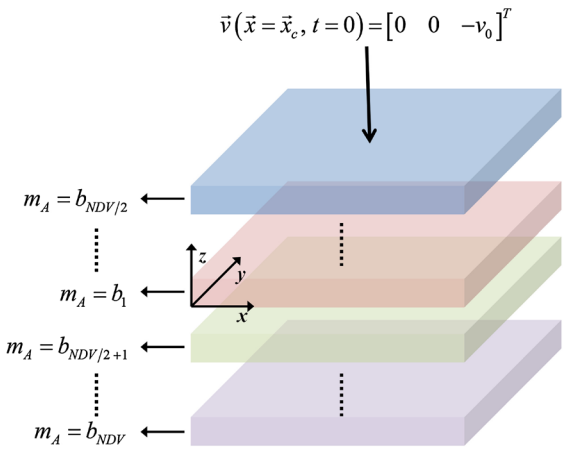

Fig. 10 Thin film of layers subjected to impulse

shown in Fig. 10. We assumed that the atoms on each layer have the same mass that is selected as a design variable. In this example, the number of atoms and design variables are 102,400 and 8, respectively. The FCC structured model consists of $40 \times 20 \times 4$ unit cells (102,400 atoms and 307,200 DOFs). The length of unit cell is about 1.5874 (nm). Both x-directional ends are gripped and the initial temperature of $T_0 = 0\ (K)$ is used. The cut-off radius is set to $r_c = 1.5r_0$, where r_0 is the equilibrium distance. For the simplicity of problem, the simulation parameters such as m, ε, σ are equally set to 1.0. All the artificial simulation parameters used in this example are identical to those used for the FCC crystal in the reference (Park et al. 2005). Thus, the size of time step is determined as $\Delta t = 10^{-2}\ (ps)$. The norm of atomic displacement vector from the MD simulation is contoured in Fig. 11. Due to the impulse and the gripped boundary, the displacement wave is oscillating.

Consider the kinetic energy of thin film at terminal time of $t_T = 500\Delta t$ as a performance measure.

$$\psi = \frac{1}{2}\dot{\mathbf{u}}^T \mathbf{M}_A(\mathbf{b})\dot{\mathbf{u}}\Big|_{t=t_T} \tag{26}$$

The analytical sensitivities obtained from the DDM using Eq. (9) and the AVM using Eq. (18) are compared in Table 7, where excellent agreements are observed for all the design variables. Also, additional computing costs required for the computation of analytical design sensitivities are listed in Table 8. For 8 design variables, the AVM requires

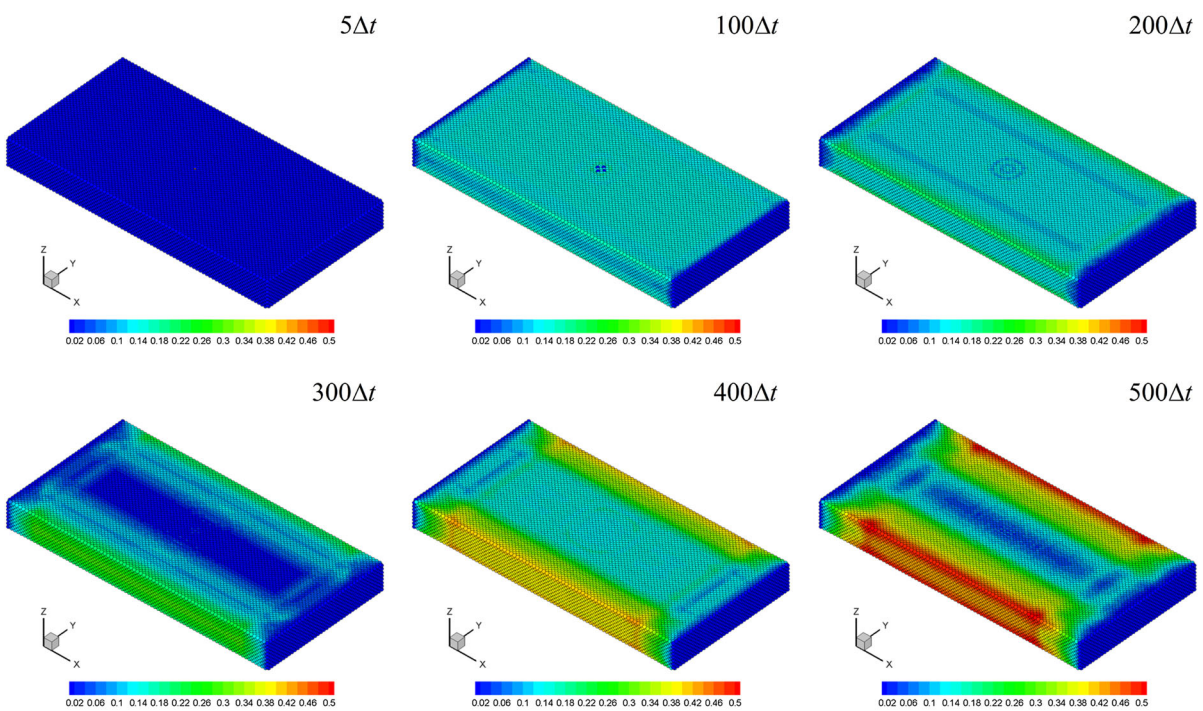

Fig. 11 Displacement contour of thin film problem. (Color figure online)

Table 7 Comparison of analytical design sensitivities

DV	(a) FDM	(b) AVM	$(b)/(a) \times 100\,\%$
b_1	7.168300E+01	7.168300E+01	100.000
b_2	−1.102679E+03	−1.102679E+03	100.000
b_3	−7.245345E+02	−7.245345E+02	100.000
b_4	−1.557312E+03	−1.557312E+03	100.000
b_5	6.936290E+01	6.936290E+01	100.000
b_6	−1.115642E+03	−1.115642E+03	100.000
b_7	−7.687209E+02	−7.687209E+02	100.000
b_8	−1.772634E+03	−1.772634E+03	100.000

Table 8 Additional computation time

	Analysis	DDM	AVM
Time (s)	11457.63	99919.35	13365
Normalized	1.0000	8.7208	1.1665

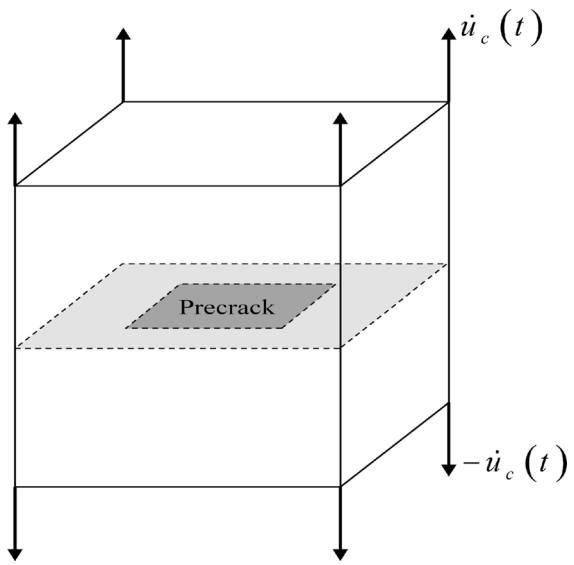

Fig. 12 Problem definition of dynamic crack propagation

only 1.16 times of analysis time whereas the DDM needs 8.72 times. Hence, for the design problems of many design variables, the AVM is more efficient than the DDM.

4.3 Dynamic crack propagation

Consider the MD simulation for the dynamic crack propagation of general FCC solid structures presented by Liu et al. (2006). The purpose is to demonstrate the efficiency of the proposed adjoint DSA method for the problem that has many design variables. The problem definition of dynamic crack propagation is illustrated in Fig. 12. A pre-crack is positioned in the center of FCC structure by eliminating the atoms in the dark gray region. The LJ 6-12 potential is utilized and the crack opens due to the constant velocity imposed on the top and bottom planes. The constant velocity is taken as $\dot{u}_c(t) = 0.5\ (nm/ps)$. The cut-off radius is determined as $r_c = 1.5r_0$ and the simulation parameters such σ, ε, and all atomic masses are taken to be unity. The MD simulation includes 255, 424 atoms under the condition of nearest-neighbor interaction only. The step size of time is $\Delta t = 10^{-2}\ (ps)$ as used in the previous example and the terminal time is $t_T = 1,000\Delta t$. The time history of crack propagation simulation is shown in Fig. 13, where the only atoms that have potential energy greater than 80 percent of the equilibrium value are contoured in Fig. 13. This technique is utilized to highlight the defective parts of lattice as the crack propagates. Notice that the potential energies of atoms near the pre-crack become larger as the crack propagates.

Consider the performance measure of potential energy summed over all atomic bond pairs at terminal time.

$$\psi = U(\mathbf{b},\mathbf{u}) = \sum_{i\neq j} 4\varepsilon \left(\left(\frac{\sigma}{r_{ij}(\mathbf{u})} \right)^{12} - \left(\frac{\sigma}{r_{ij}(\mathbf{u})} \right)^{6} \right) \Bigg|_{t=t_T}, \tag{27}$$

where the total number of atoms is $N_a = 255,424$. Design variables are the mass of each atom except atomic mass on the boundary. Thus, the total number of design variables is 249,024. The adjoint DSA

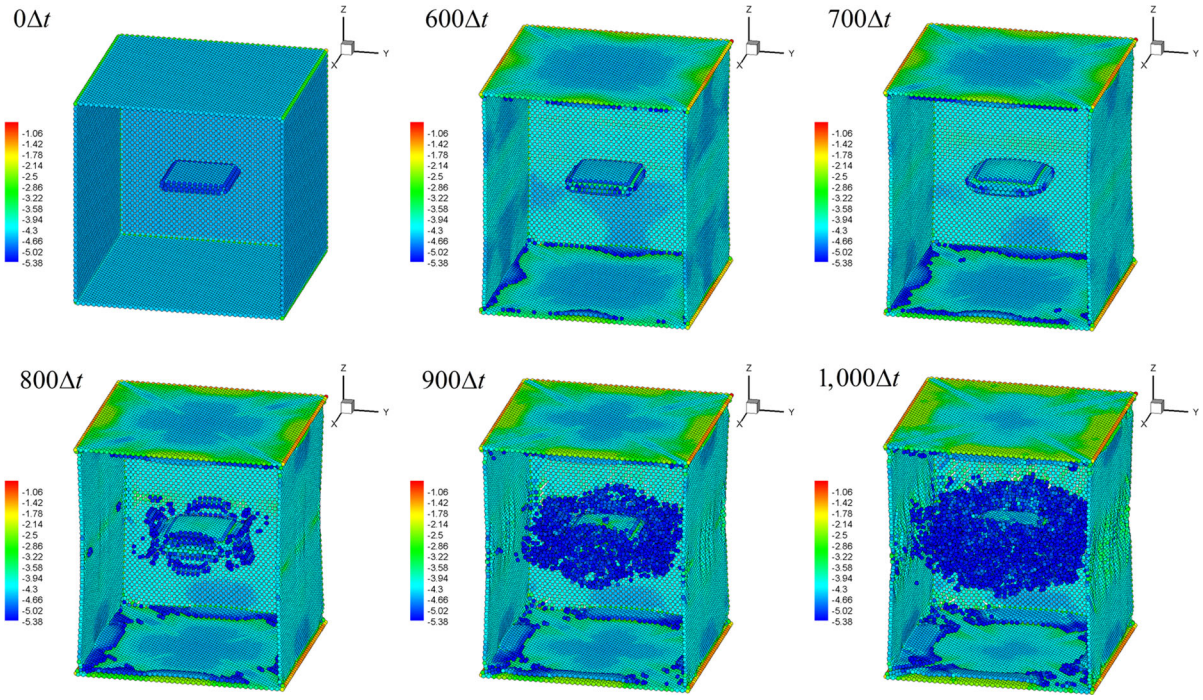

Fig. 13 Analysis results for 3D MD crack propagation. (Color figure online)

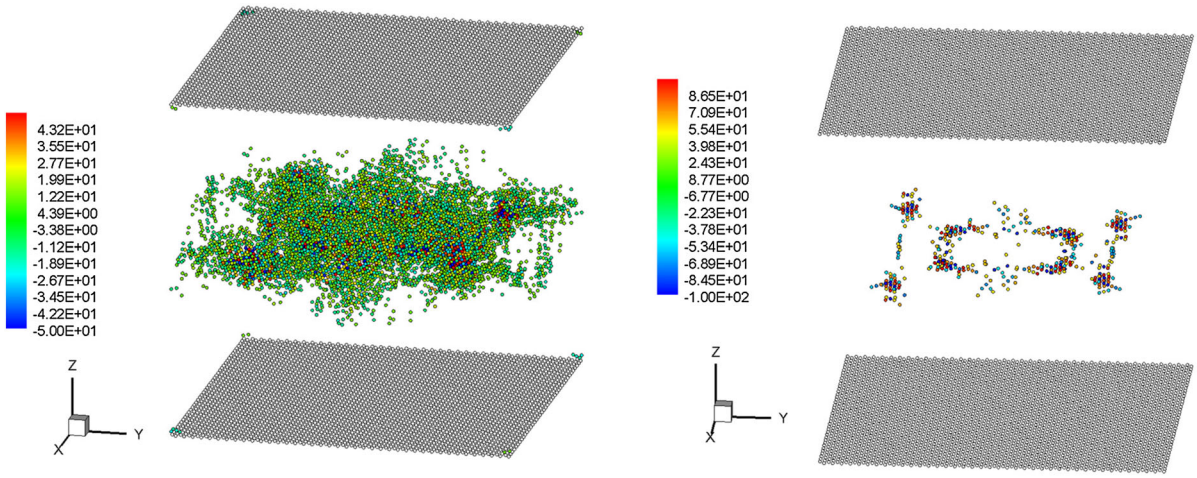

Fig. 14 Contour of selected atoms whose design sensitivity is greater than (L: 10, R: 50). (Color figure online)

results are shown in Fig. 14, where some highly sensitive atoms are plotted for visualization purpose. High sensitivity is observed at the atoms where the bond breaks as crack propagates. Required computational costs for the MD simulation, AVM, and FDM are listed in Table 9. About 1.1 times of MD simulation time is additionally required to obtain the adjoint sensitivities with respect to 0.25 million design variables. If the FDM is employed, about 3,000 years are additionally necessary to obtain the equivalent sensitivities. Even though the AVM requires more storage space to keep all the time history of solutions,

Table 9 Comparison of computational costs

Time	MD Simulation	AVM
Computation (s)	373,253.1	405,524.5
Computation	4 days 8 h	4 days 17 h
Normalized	1.0000	1.0865

the AVM is appropriate and indispensable in the DSA of MD systems that include a huge number of design variables.

5 Conclusions

In the parallel computation environment, a DSA method for MD simulations is developed using the adjoint approach. To overcome the difficulty of computational costs, a spatial decomposition method is used for the original response as well as the sensitivity analyses in parallel computation. Assigning each processor a fixed spatial region and exchanging data using the known atomic positions, the communication cost is minimized compared with other parallel computing algorithms such as the atomic and the force decomposition methods. Numerical implementation demonstrates that the developed adjoint DSA method is not only accurate for highly nonlinear design problems but also very efficient for large scale problems. The developed adjoint DSA method for MD simulations is applicable for emerging nanotechnology problems such as the design of nanoparticles, nanoscale sensors, ultra-strength materials, drug delivery matter, and so on.

References

Black, J., Bopp, P.: The vibration of atoms at high miller index surfaces: face centred cubic metals. Surf. Sci. **140**(2), 275–293 (1984). doi:10.1016/0039-6028(84)90733-7

Cho, S., Choi, KK.: Design sensitivity analysis and optimization of non-linear transient dynamics. Part I: Sizing design. Int. J. Numer. Meth. Eng. **48**(3):351–373 (2000). doi:10.1002/(SICI)1097-0207(20000530)48

Cho, S., Choi, KK.: Design sensitivity analysis and optimization of non-linear transient dynamics. Part II: Configuration design. Int. J. Numer. Meth. Eng. **48**(3):375–399 (2000). doi:10.1002/(SICI)1097-0207(20000530)48

Choi, K., Kim, N.: Structural Sensitivity Analysis and Optimization, vol. 1. Springer, New York (2005)

Farrell, D.E., Park, H.S., Liu, W.K.: Implementation aspects of the bridging scale method and application to intersonic crack propagation. Int. J. Numer. Meth. Eng. **71**(5), 583–605 (2007). doi:10.1002/nme.1981

Gao, Z., Ma, Y., Zhuang, H.: Optimal shape design for the time-dependent Navier–Stokes flow. Int. J. Numer. Meth. Fluid **57**(10), 1505–1526 (2008). doi:10.1002/fld.1673

Hsieh, C., Arora, J.: Design sensitivity analysis and optimization of dynamic response. Comput. Meth. Appl. Mech. Eng. **43**(2), 195–219 (1984). doi:10.1016/0045-7825(84)90005-7

Kadowaki, H., Liu, W.K.: Bridging multi-scale method for localization problems. Comput. Meth. Appl. Mech. Eng. **193**(30–32), 3267–3302 (2004). doi:10.1016/j.cma.2003.11.014

Kim, MG., Jang, H., Kim, H., Cho, S.: Multiscale adjoint design sensitivity analysis of atomistic-continuum dynamic systems using bridging scale decomposition. Model. Simul. Mater. Sci. Eng. **21**(3):035,005 (2013)

Kim, M.G., Jang, H.L., Cho, S.: Adjoint design sensitivity analysis of reduced atomic systems using generalized Langevin equation for lattice structures. J. Comput. Phys. **240**(0), 1–19 (2013). doi:10.1016/j.jcp.2013.01.020

Lamb, J.S.W., Roberts, J.A.G.: Time-reversal symmetry in dynamical systems: a survey. Phys. D **112**(1–2), 1–39 (1998). doi:10.1016/S0167-2789(97)00199-1

Leach, A.R.: Molecular Modelling: Principles and Applications. Pearson Education, Prentice Hall (2001)

Liu, W.K., Karpov, E.G., Park, H.S.: Nano Mechanics and Materials. Wiley, New York (2006)

Mendelev, M., Han, S., Srolovitz, D., Ackland, G., Sun, D., Asta, M.: Development of new interatomic potentials appropriate for crystalline and liquid iron. Philos. Mag. **83**(35), 3977–3994 (2003)

Park, H.S., Karpov, E.G., Klein, P.A., Liu, W.K.: Three-dimensional bridging scale analysis of dynamic fracture. J. Comput. Phys. **207**(2), 588–609 (2005). doi:10.1016/j.jcp.2005.01.028

Plimpton, S.: Fast parallel algorithms for short-range molecular dynamics. J. Comput. Phys. **117**(1), 1–19 (1995). doi:10.1006/jcph.1995.1039

Spohr, E., Heinzinger, K.: Molecular dynamics simulation of a water/metal interface. Chem. Phys. Lett. **123**(3), 218–221 (1986). doi:10.1016/0009-2614(86)80016-1

Strogatz, S.H.: Nonlinear Dynamics and Chaos, 1st edn. Perseus Books Group, Cambridge (1994)

Tadmor, E.B., Phillips, R., Ortiz, M.: Mixed atomistic and continuum models of deformation in solids. Langmuir **12**(19), 4529–4534 (1996). doi:10.1021/la9508912

Tortorelli, D.A., Haber, R.B., Lu, S.C.Y.: Design sensitivity analysis for nonlinear thermal systems. Comput. Meth. Appl. Mech. Eng. **77**(1–2), 61–77 (1989). doi:10.1016/0045-7825(89)90128-X

Tsay, J., Arora, J.: Nonlinear structural design sensivitity analysis for path dependent problems. Part 1: General theory. Comput. Meth. Appl. Mech. Eng. **81**(2), 183–208 (1990). doi:10.1016/0045-7825(90)90109-Y

Tuckerman, M., Berne, B.J., Martyna, G.J.: Reversible multiple time scale molecular dynamics. J. Chem. Phys. **97**(3), 1990–2001 (1992). doi:10.1063/1.463137